Development of an Oxygen Sensitive Model Gel System to Detect Defects in Metal Oxide Coated Multilayer Polymeric Films

Ashutos Parhi, Kanishka Bhunia, Barbara Rasco, Juming Tang, and Shyam S. Sablani

Abstract: Metal oxide coated multilayered polymeric pouches provide a suitable alternative to foil-based packaging for shelf-stable products with extended shelf-life. The barrier performance of these films depends upon the integrity of the metal oxide coating which can develop defects as a result of thermal processing and improper handling. In this work, we developed a methodology to visually identify these defects using an oxygen-sensitive model gel system. Four pouches with different metal oxide coatings: **MOA** (Coated PET), **MOB** (SiO_x-coated PET), **MOC** (Overlayer-AlO_x-Organic-coated PET), **MOD** (Overlayer-SiO_x-coated PET) were filled with water and retort-processed for 30 and 40 min at 121 °C. After processing, the pouches were cut open, dried and subsequently filled with a gel containing methylene blue that changes color in the presence of oxygen. The pouches were then stored at 23 and 40 °C for 180 and 90 days, respectively. Defects were identified by observing the localized color change from yellow to blue in the packaged gel. These observations were confirmed through measurement of oxygen and water vapor transmission rates, as well as SEM and CLSM analyses. The MOC pouches showed the least change in barrier properties after thermal processing. This was due to crosslinking in the organic coating and protection provided by the overlayer. The melting enthalpy of all films increased significantly ($P < 0.05$) after sterilization. This may increase the brittleness of the substrates after processing. Findings may be used to improve the barrier performance of metal oxide coated polymeric films intended for food packaging applications.

Keywords: CLSM, defects, metal oxide coating, oxygen indicator, SEM

Practical Application: In this study, we developed a methylene blue-based, oxygen-sensitive model gel system to identify defects in metal oxide coated polymeric structures induced by thermal processing and mechanical stresses. We also performed a comprehensive analysis of these defects through CLSM and SEM. The gel system and methodology developed may be useful in the design and development of high barrier metal oxide coated films.

Introduction

The demand for ready-to-eat, packaged products with an extended shelf life is ever increasing. Thermal sterilization is an effective method of producing shelf-stable food products with good quality. Flexible packaging made with aluminum foil has a very high oxygen and water vapor barrier, and therefore is commonly used to provide long shelf life to commercially sterilized foods. Unfortunately, metal foil-based packaging is not compatible with microwave-assisted thermal sterilization. Metal oxide coated multilayer polymeric films provide an excellent alternative to foil-based packaging. In addition, such packaging has a higher transparency and can pass through metal detectors while imparting very high barrier to oxygen and moisture (Byun et al., 2010; Byun, Bae, Cooksey, & Whiteside, 2010).

Several metal oxide-based coatings have been used to improve the barrier performance of multilayer polymeric films for food packaging applications. Aluminum and silicon oxides are the most common metal oxide coatings for polyethylene terephthalate (PET) and nylon. These are applied by atomic layer deposition (ALD), chemical vapor deposition (CVD), and physical vapor deposition (PVD) techniques (Struller, Kelly, & Copeland, 2014; Yanaka et al., 2001). The coating provides the primary barrier to oxygen in metal oxide coated multilayer polymeric films. In other polymer-based films, ethylene vinyl alcohol (EVOH) layer acts as the main source of barrier to oxygen (Zhang et al., 2017). However, the overall barrier performance of metal oxide coated films depends significantly upon the presence of various defects such as pinholes and cracks. These defects increase the rate of permeation of water vapor and oxygen through the packaging film (Roberts et al., 2002; Yanaka et al., 2001).

When metal oxide coated multilayer polymeric pouches are thermally sterilized, they get exposed to high temperatures in the range of 121 °C, along with high moisture and pressure. Studies demonstrate that the gas barrier properties of metal oxide coated multilayer polymeric films decrease after sterilization, due to changes in their thermal and morphological characteristics (Dhawan et al., 2014; Zhang et al., 2017). Other studies have

JFDS-2019-0374 Submitted 3/15/2019, Accepted 7/5/2019. *Authors Parhi, Tang, and Sablani are with the Dept. of Biological Systems Engineering, Washington State Univ., P.O. Box-646120, Pullman, WA 99164-6120, USA. Author Bhunia is with the Dept. of Agricultural and Food Engineering, Indian Inst. of Technology, Kharagpur, India. Author Rasco is with the School of Food Science, Washington State Univ., P.O. Box 64376, Pullman, WA 99164-6376, USA. Direct inquiries to author Sablani (E-mail: ssablani@wsu.edu).*

Disclaimer: Dr. Bradley W. Bolling served as Scientific Editor and Professor Julie M Goddard as Associate Editor overseeing single-blinded review of this manuscript. It is the policy of JFS to blind Editorial Board members from the peer-review process of their own submissions, just as all authors are blinded.

doi: 10.1111/1750-3841.14755

Journal of Food Science A Publication of the Institute of Food Technologists

Table 1–Structural information of metal oxide coated pouches.

Pouch type	Thickness (μm, $N = 5$)	Layer composition[a]	Dimension (cm × cm)	Shape	Gel Volume (mL)
MOA	92.6 ± 0.9	Coated PET (12 μm)*//ONy (15 μm)//CPP(50 μm)	18.5 × 13	Stand-up	400
MOB	95 ± 0.5	SiO_x-coated PET (12 μm)//ONy (15 μm)//CPP(60 μm)	17 × 13	Flat	300
MOC	83 ± 0.5	**Overlayer/AlO_x -Organic-coated PET (13 μm)//ONy (15 μm)//CPP (50 μm)	18 × 13	Flat	350
MOD	92 ± 0.7	Overlayer/SiO_x-coated PET (12 μm)//ONy (15 μm)//CPP(60 μm)	18 × 13	Stand-up	350

[a]ONy: Oriented Nylon 6; CPP: Cast Polypropylene
*Information related to the type of metal oxide coating is not available for this pouch.
**Organic coating is composed of modified Poly Acrylic Acid (PAA) layer of 1 μm thickness and present on AlO_x-coated PET layer of 12 μm thickness.

examined the barrier performance of metal oxide coating itself along with external factors that may lead to defects (Leterrier, Månson, & Wyser, 2001; Rochat, Leterrier, Fayet, & Månson, 2005; Singh et al., 2007; Struller et al., 2014). However, these studies have analyzed the performance of the coatings present on the exterior surface of films (Dhawan et al., 2014; Zhang et al., 2017), or of films that were not exposed to commercial sterilization conditions such as heating at 121 °C under high moisture (Leterrier et al., 2001; Struller et al., 2014). Research is needed to develop an effective method to identify the changes in coating layer of metal oxide coated multilayer polymeric films after thermal processing.

Several techniques including scanning electron microscopy (SEM), transmission electron microscopy (TEM) and atomic force microscopy (AFM), have been used to characterize the nature and magnitude of defects occurring in the AlO_x or SiO_x based coatings (Charifou, Espuche, Gouanvé, Dubost, & Monaco, 2016; Leterrier et al., 2001; Roberts et al., 2002; Struller et al., 2014; Yanaka et al., 2001). These traditional characterization techniques require samples with very small dimensions that are usually cut from a large area of a coated film. The dimensions of defects in metal oxide coated films are very small (with at least one dimension in microns). The locations of these defects are also unknown. Therefore, a large number of samples is needed for analysis, which is time consuming. Furthermore, metal oxide coatings are generally located underneath the top PET layer and are laminated with PP and nylon layers to minimize the effects of mechanical stress-initiated cracking. This also makes it difficult to detect the defects. Therefore, it is important to develop a method to identify defects within the coating and their location for subsequent characterization.

An oxygen indicator can be used to identify defects in metal oxide coated multilayer polymeric films. One of the most effective methods is the use of OxyDot (Oxysense®, New Castle, DE), which can non-invasively measure the oxygen content inside of a sealed package (Bhunia, Sablani, Tang, & Rasco, 2016). Ruthenium, palladium or platinum-based chemical complexes that work on the principle of luminescent quenching and embedded in an organic or inorganic polymer matrix with permeability to oxygen, can also be used to detect oxygen ingress inside of a packaging.

Other examples of oxygen-sensitive indicators include colorimetric materials such as myoglobin-based reagents, redox dyes such as methylene blue incorporated into pellets, and dyes activated by UV light (Mills, 2005). The reaction between the dye and oxygen can be irreversible, and the intensity of resulting color change varies with the level of oxygen present. These techniques work well to detect the oxygen ingress through a film or oxygen present inside a package. However, these methods have been less successful in identifying localized defects in packaging. Since these detectors are very small in size, it is very challenging to identify the location of defects in the metal oxide coating of commercial pouches. Some indicators are also sensitive to light, reducing applicability of those indicators (Mills, 2005).

Kass and Darby (2010) developed an oxygen-sensitive gel based on methylene blue dye to analyze barrier deterioration in multilayer films. Using the gel system, they examined multilayer film structures containing EVOH, nanocomposites, silicon and aluminum oxide coatings as well as aluminum foil-based packaging materials for defects after retort process. The gel showed a color change due to oxygen ingress, indicating defects in coating and lamination. However, the change in total color had a poor correlation with changes in oxygen transmission rate (Kaas & Darby, 2010). In addition, the gel had a highly alkaline formulation (pH: 11 to 14), making it unstable. The authors also did not characterize the nature of defects that caused the film barrier to deteriorate.

The main objectives of our study were to formulate a suitable oxygen sensitive gel system that can be used to identify and characterize defects in metal oxide coated multilayer films, as well as visually analyzing the coating performance. To reduce the time needed to identify defects, we tested the gel system at elevated temperatures. We further characterized defects using SEM and confocal laser scanning microscope (CLSM).

Materials and Methods

Multilayer pouches and thermal processing

We selected four types of multilayer film pouches for this study. Table 1 presents their structures, dimensions, and thicknesses. The pouches filled with 250 to 350 mL of MilliQ water (Millipore Corporation, Billerica, MA) as food simulant were vacuum packed and processed in a retort (Allpax Products, LLC, Seymour Meyers Blvd., LA) for 30 min (R30) and 40 min (R40) at 121 °C. Processing times were selected based on an expected target lethality (F_0) of 6 to 9 min for solid foods in flexible pouches (Mohan, Ravishankar, Bindu, Geethalakshmi, & Srinivasa Gopal, 2006). The retort come-up time was set to 10 min, while the pressure and atmospheric cool times were kept at 5 and 2 min, respectively. After processing, the pouches were emptied, dried and refilled with an oxygen sensitive model gel system for detection of defects.

Preparation of oxygen sensitive gel

We prepared the oxygen sensitive gel by combining anhydrous dextrose (D+ Glucose; molecular weight: 180.16 g/mol; melting point: 150 to 152 °C), sucrose fatty acid ester, agar (pH: 5 to 8, gel point: 35 to 37 °C, melting point: 70 °C, gel strength: >300 g/cm^2), sodium hydroxide (free flowing pellets;

molecular weight: 39.9 g/mol) and methylene blue trihydrate (molecular weight: 373.9 g/mol). Dextrose, agar, methylene blue trihydrate and sodium hydroxide were purchased from Sigma-Aldrich (Millipore Sigma, St. Louis, MO, USA) and sucrose was procured from TCI chemicals (TCI Chemicals, Portland, OR, USA).

The agar gel system functions based on the reaction between active compounds such as glucose, methylene blue, sodium hydroxide and oxygen. The development of blue color in the gel is caused by oxidation of methylene blue upon exposure to atmospheric oxygen (Campbell, 1963). Initially, glucose present in the aqueous solution tends to react with the hydroxide ion from NaOH to form glucoside ions (Campbell, 1963). In the second step, methylene blue added to the solution is oxidized by the dissolved oxygen in the solution and attains its blue form (Campbell, 1963; Kaas & Darby, 2010). Simultaneously, it also reacts with the glucoside ions and, in the process, undergoes reduction (Campbell, 1963). Subsequent exposure to oxygen re-oxidizes it, leading to the formation of the blue color. However, the process continues until all the glucoside ions are consumed (Campbell, 1963; Kaas & Darby, 2010).

To prepare the dye, MilliQ water (Millipore Corporation, Billerica, MA) was boiled for 20 min to reduce the dissolved oxygen. Subsequently, the water was cooled to 85 °C by flushing nitrogen (99% purity) with high stirring. This helped reduce the headspace air in the beaker and prevented more oxygen from dissolving in the water during cooling. The beaker was also covered with aluminum foil to reduce exposure to oxygen during the experiment. The water temperature was carefully maintained and measured with a T type thermocouple (Omega engineering, Inc., Norwalk, CT, USA). At this stage, the chemicals were added to the hot water. The gel system was prepared by dissolving 0.1 g of sucrose fatty acid ester, 1.5 g of agar, 0.05 g of sodium hydroxide, 0.015 g of methylene blue and 6 g of D+ glucose per 100 mL of water. At first, one third of the D+ glucose (2 g) was mixed properly with sucrose fatty acid ester (0.1 g) to limit the formation of agglomerates. The mixture was then poured into deoxygenated hot water (85 °C) and allowed to mix for 5 min using a magnetic stir-plate at 700 rpm. The remaining glucose (4 g) was subsequently added to the solution at the same rpm.

After proper dissolution of glucose and sucrose, agar powder (1.5 g) was added to the solution. The addition of agar caused the solution viscosity to increase and to prevent the formation of any lumps, stirring speed was gradually increased to 1100 rpm. After 5 min, sodium hydroxide (0.05 g) was added to the solution. The color of the mixture gradually changed from light gray to light yellow. With further stirring, it changed to deep yellow. The mixture was stirred for another 5 min before methylene blue (0.015 g) was added. This was further stirred for 10 more min at 1100 rpm, and quickly poured into retort-processed pouches. The gel filled pouches were sealed using an impulse sealer with 4 to 5 s of dwell time. Depending on the pouch size and shape, the volume of packaged gel-water system varied (Table 1).

The pouches were filled with little to no headspace to minimize atmospheric oxygen inside the pouch. They were subsequently cooled down and stored at 23 and 40 °C for 180 and 90 days, respectively at atmospheric oxygen environment (21 % oxygen) and 25 ± 4% relative humidity. Unprocessed pouches were also filled with the gel in a similar manner and stored at the same conditions. Four replicates of gel filled pouches were prepared from each of the metal oxide coated structures for each of the unprocessed (control) and retort processed (30 min (R30) and 40 min (R40)) and for each of the two selected temperatures (23 and 40 °C). Four replicate images were taken at every 15- and 30-day intervals for samples stored at 40 °C and for 23 °C, respectively beginning from day 0 till the end of their respective storage periods.

The pH of the gel-forming solution was measured using a lab scale Mettler-Toledo pH meter at 23 and 40 °C. The moisture content of the gel was measured by drying 5 g of solid gel in a hot air oven at 55 °C for 72 hr (Brown, Fryer, Norton, & Bridson, 2010). The water activity was measured by analyzing 2 g of gel sample in an AqualabPre water activity meter (Meter Food, Pullman, WA, USA) at 25 °C. At the end of storage, we extracted film samples for SEM and CLSM analyses from the locations in the gel filled pouches that changed color from yellow to blue due to oxygen ingress.

Oxygen and water vapor transmission rates

To determine the effects of thermal processing on the barrier properties of the pouches, the oxygen transmission rates (OTRs) were measured with the MOCON Ox-Tran 2/21 MH permeability instrument (Modern Control, Minneapolis, MN, USA) as per ASTM F 1927. The test conditions were set at 23 °C, 1 atm pressure and 55 ± 1% relative humidity (RH). The water vapor transmission rates (WVTRs),on the other hand, were measured as per ASTM F 372–99 at 100% RH and 38 °C, using Permatran 3/33 MG model (Modern Control). Films with 50 cm^2 surface area were extracted from pouches before and after sterilization and mounted onto the instruments. Samples were measured in triplicates for both tests.

Thermal analysis

The changes in polymer melting and cold crystallization enthalpies as a result of thermal processing were determined by modulated differential scanning calorimetry (MDSC) (Model Q2000, TA instruments, New Castles, DE, USA). Film samples weighing 10.3 ± 0.7 mg each, extracted from pouches before and after sterilization, were heated from −30 to 300 °C with a heating rate of 1 °C/min and modulation amplitude of ± 0.159 for every 60 s. Thermograms were analyzed for enthalpies of melting and cold crystallization using instrument software (Universal Analysis, TA Instruments). The enthalpy of crystallinity was calculated for all samples before and after thermal processing by considering the changes that occurred at the same temperature range in both the reversing and nonreversing components of the signal (Bhunia et al., 2016).

Scanning electron microscope

Film samples measuring 5 mm × 5 mm were cut from different locations in the pouches with blue marks and dried at 23 °C for 12 h in a vacuum desiccator. Once dried, the samples were adhered to aluminum stubs with carbon tabs and gold-coated under high vacuum by a sputter coater (Technics Hummer V gold sputter coater, Hummer 6.6 Sputter system, CA) to obtain a coating thickness of 7 to 10 nm. The gold coated samples were imaged in an SEM (FEI Quanta 200F, Thermo Scientific™ Quanta™, Hillsboro, OR, USA) at 20 KV accelerating voltage and a spot size of 3.0 in ETD detector mode under high vacuum. Both the outer (PET) and inner (PP) layers of the films were examined. All the measurements were performed in duplicates ($N > 20$).

Confocal laser scanning microscope

Leica TCS SP8 X laser scanning confocal microscope (CLSM) (Leica Microsystems Inc., Buffalo Grove, IL, USA) was used to

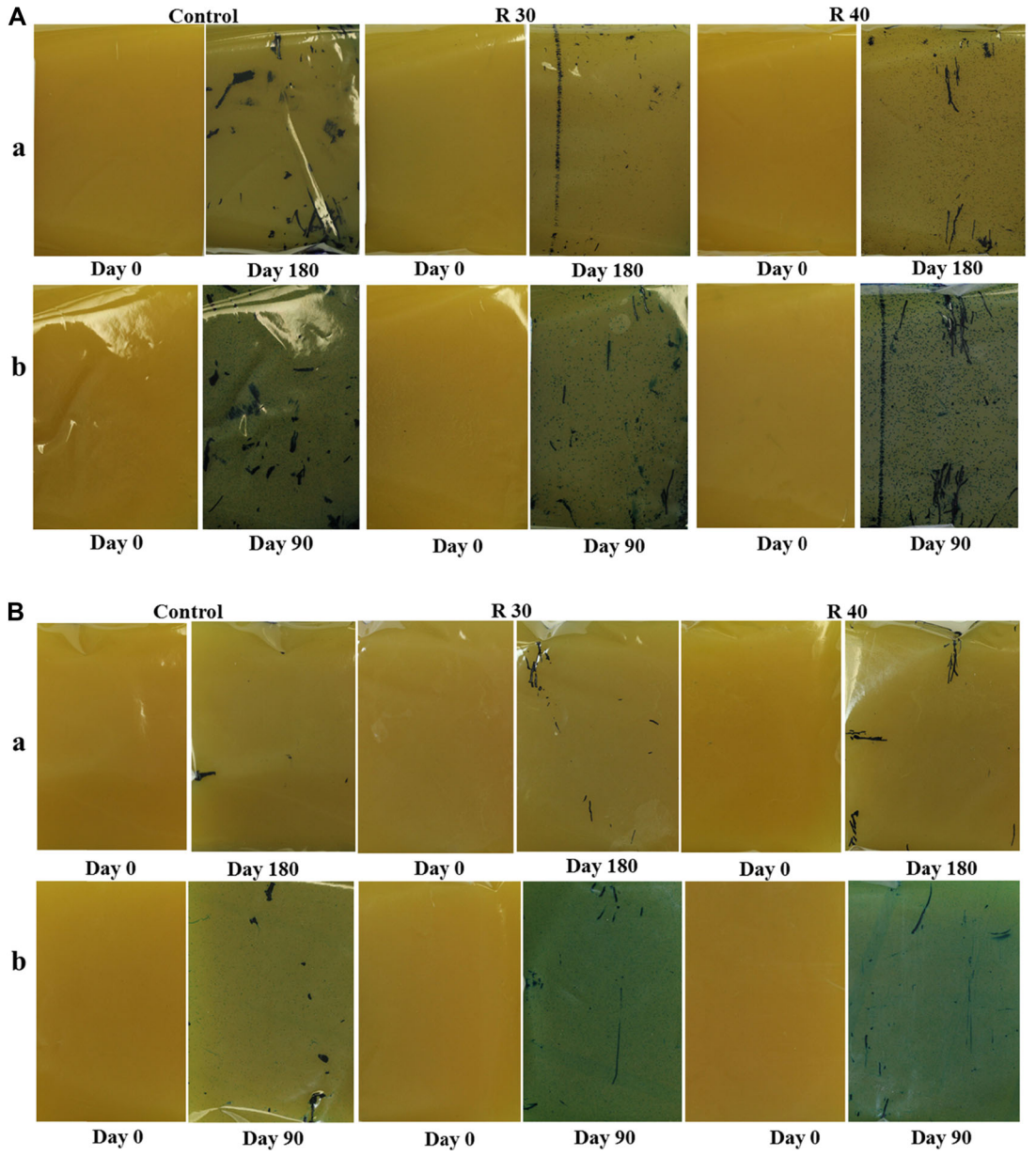

Figure 1–Color change in model gel filled (A) MOA; (B) MOB; (C) MOC; and (D) MOD pouches at (a) 23 °C and (b) 40 °C for control, retort 30 (R30) and 40 min (R40), respectively.

analyze defects in the metal oxide coating. Since the coating layer is present underneath the PET layer, confocal microscopy was performed by exposing PET surface of the multilayer film sample toward the incident laser radiation. Samples of 10 mm × 10 mm were collected from several affected locations with a blue color and mounted on a glass slide. This was covered with immersion oil (Leica type F immersion fluid, ISO 8036) and a cover slip which was glued in place with an UV curable adhesive. The white light laser was used for imaging. Images with the reflectance mode were taken at 496 nm with a hybrid detector and transmittance images were procured with a PMT detector. All imaging was performed with a dry 20 X objective (N.A.: 0.75). For pouches stored at 23 °C, the transmittance mode was used and for 40 °C storage samples, the reflectance mode was employed due to the greater intensity of blue color in those samples which hindered the effective detection of defects in transmittance mode. Overall, the transmittance mode was more effective in identifying the nature of defects in film samples. Images were collected in 3D Z-stack as well as the 2D modes in order to determine whether the defects were two-dimensional (2D) or had a depth associated with them. All measurements were performed in duplicates ($N > 20$).

Data analysis

A two-way completely randomized design with Tukey's HSD was performed using SAS 9.4 to analyze changes in polymer enthalpies as well as film OTR and WVTR data. The experimental values were compared in order to identify significant differences ($P < 0.05$) in the above-mentioned properties for the pouches before and after thermal sterilization.

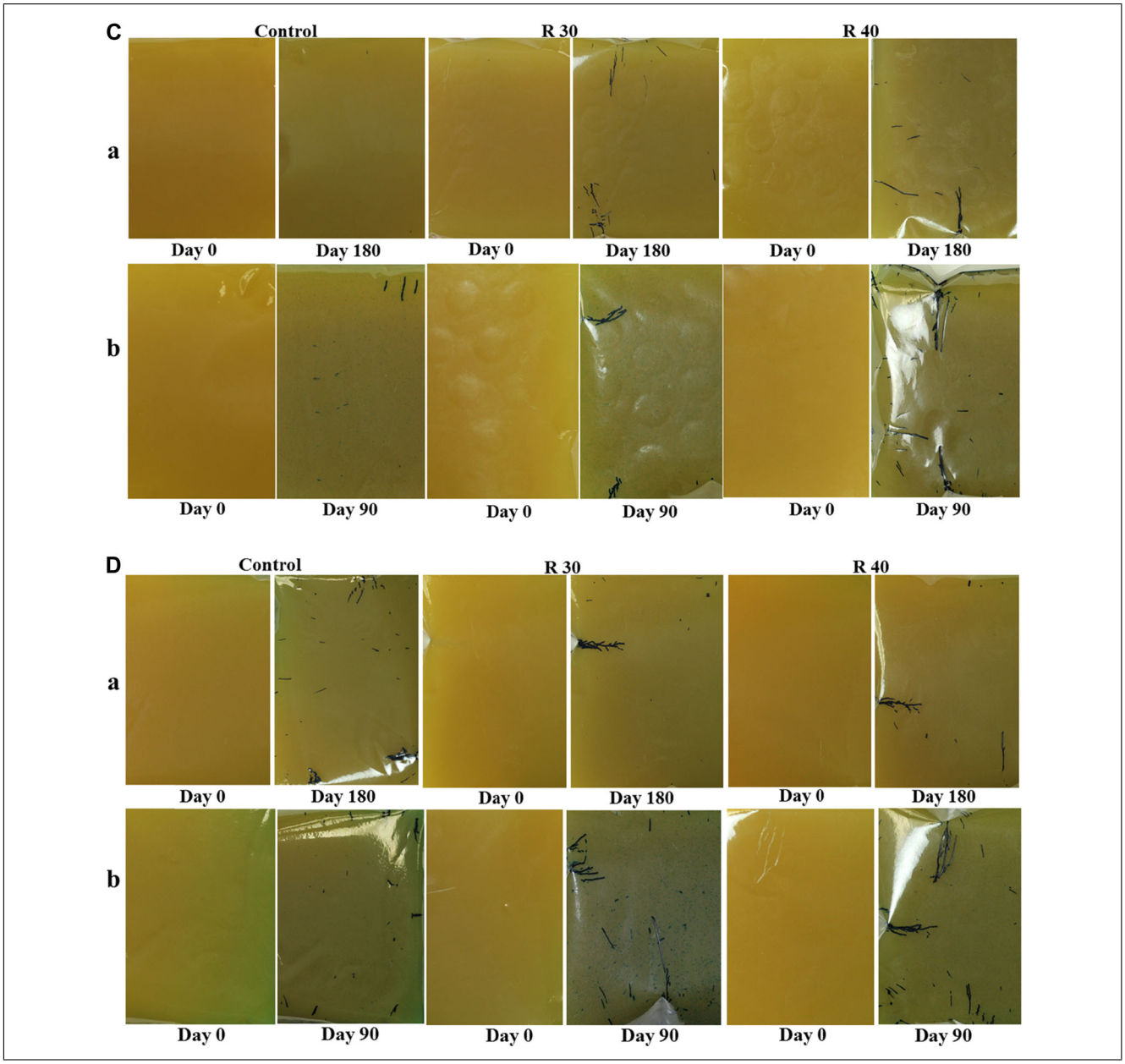

Figure 1–*Continued.*

Results and Discussion

Effectiveness of the gel method for detecting defects

Figure 1 shows development of the blue color in the gel packed into different pouches due to oxygen ingress for two storage temperatures. The darker blue spots in Figure 1 indicate the most affected locations, with higher oxygen permeations. Note that the unprocessed (control) pouches also developed a blue color during storage. This indicates the presence of defects in the coating layer even before exposure to sterilization conditions. However, there was more damage to the coating in thermally processed pouches, as indicated by the increased color change in the gel (Figure 1). Furthermore, the level of change in gel color from yellow to blue varied by pouch type and storage temperature. More change occurred in pouches with higher oxygen permeability, as well as those stored at 40 °C as compared to 23 °C.

Amongst the four pouches, MOA showed the highest change in gel color overall, while MOC showed the least (Figure 1). The MOA pouch also showed most defects while the MOC pouch had least number of defective sites as indicated by the locations with blue coloration (Figure 1). As explained in Section 3.2, the overall change in gel color depended on the respective OTRs of individual pouches. The blue color development was more intense in pouch regions having temperature and stress-induced defects as a result of exposure to thermal processing and handling. This may be due to higher oxygen ingress at these locations. Pouches processed for 40 min showed a higher color change than unprocessed (control) and 30-min processed samples. This suggests that the barrier properties deteriorated more with longer thermal treatment. The pH of the gel forming solution was 7.21 ± 0.01 and 6.55 ± 0.05 at 40 and 23 °C, respectively. The moisture content and water activity of the gel were 91.6 ± 0.6% and 0.987 ± 0.001, respectively. The

agar acted as an excellent host for the active chemical compounds due to its gel forming capabilities. It also restricted diffusion of color compounds (oxidized methylene blue) throughout the system, while providing an inert matrix. The use of sucrose fatty acid ester on the other hand helped to reduce syneresis in agar while helping maintain a stable pH (Nishinari & Fang, 2016).

As explained earlier, the development of blue color in the gel system was induced by oxidation of methylene blue present in the gel upon exposure to atmospheric oxygen (Campbell, 1963). In the packaged gel, the color change occurred faster at sites with higher barrier deterioration (Figure 1) as this exposed the gel to higher amount of oxygen as compared to locations with lesser deterioration in metal oxide coating. The color change in methylene blue from no blue (reduced form) to blue (oxidized form) continued until all the glucoside ions were consumed at the affected locations (Campbell, 1963; Kaas & Darby, 2010). Defects in coating layer of the pouches initially allowed oxygen to permeate through, and glucoside ions in the gel matrix kept the methylene blue reduced as soon as it was oxidized by the permeated oxygen. The color change in methylene blue became irreversible once glucoside ions were depleted, resulting in a permanent blue coloration at sites with barrier deterioration (Campbell, 1963; Kaas & Darby, 2010).

Results show that the color change happened in the gel surface that was directly in contact with inner layer (PP), as well as within the layer of film structure itself. The color change first occurred within the film and in the gel entrapped at the defects in PP and later in the gel surface in contact with the defective layer. Microscopic images in Figure 2 indicate defects in the PP layers. When the liquid gel was hot filled into pouches, it possibly entered these defects. Upon cooling, the solidified gel may have been trapped at those locations. When the trapped gel encountered the permeated oxygen, it changed color from yellow to blue. As these defects were found to be present across the PP layer of the entire pouch (Figure 2), wherever the barrier deterioration took place, it resulted in color change of the entrapped gel. This facilitated the identification of the defective sites. On the other hand, the color change in the gel surface may have occurred when glucoside ions at these defects were consumed, allowing oxygen to diffuse through and react with the surface layer of the gel underneath. This surface color change was more pronounced in pouches stored at 40 °C than at 23 °C. Finally, methylene blue tends to adsorb into polypropylene surfaces which may have also led to a color change in the film as well (Bélaz-David et al., 1997).

The higher color change in pouches stored at 40 °C compared to 23 °C may be attributed to two major factors: (1) the diffusion of oxygen and related reactions within the gel matrix and (2) the diffusion of the blue color itself from the surface to the core of the gel. The pouches stored at 40 °C had higher oxygen ingress due to an increase in the OTRs of polymeric films at higher temperatures (Henry et al., 2001). Oxygen diffusivity in agar increases with temperature (Bhunia et al., 2016). Initially, oxygen permeated from the outside underwent dissolution at the gel surface (Bhunia et al., 2016), leading to reaction with the dye and generation of blue color. Subsequently, the dissolved oxygen diffused through the gel matrix, changing the color from yellow to blue. At 40 °C, the oxygen diffusivity in gel may have increased significantly, increasing the blueness of the gel. Therefore, one reason for the higher color change at 40 °C may be the diffusion-reaction process.

The other factor may be the diffusion of the blue color itself across the gel matrix. All four types of pouches stored at 40 °C showed a release of water from the gels. Storage at temperature above the gelation temperature (35 to 37 °C) of agar may have weakened the junctions in its structure resulting in increased syneresis (Walstra, 2003). As the agar gel is composed of entrapped water molecules within its crosslinked network (moisture content of the gel was 91.6 ± 0.6%), exposure to high storage temperatures would promote water release. This would allow higher diffusion of blue color, aided by the movement of water molecules in the gel. The pouches used in this study showed low WVTRs (Table 2), which limited moisture loss. Therefore, storage at elevated temperatures would lead to higher diffusion of the blue color throughout the gel matrix, assisted by the water released. Agar also has a porous structure (Ackers & Steere, 1962; Pernodet, Maaloum, & Tinland, 1997), which may have allowed the blue color to permeate through the gel structure. These factors collectively allowed the oxidized methylene blue to diffuse from the affected regions to the rest of the gel making it difficult to identify defects. This effect was much more pronounced in structures with high OTRs (Table 2), as higher oxygen permeation led to increased blue coloration.

Despite the drawbacks associated with agar's lower gelation temperature, testing for defects at higher storage temperatures has advantages. With increased permeation through packaging and diffusion of oxygen at 40 °C, it is faster to identify defective regions compared to samples stored at 23 °C (Figure 1). The color change also correlated well with the postprocessing OTRs of the respective pouches (Table 2). The MOA pouches with highest OTR showed a maximum color at the end of storage. However, a polymer gel matrix with a higher gelation temperature could further accelerate the identification of defects in the metal oxide coating by storing the pouches at elevated temperatures.

Oxygen and water vapor transmission rates

All four films had very low OTRs ($\leq 0.04 \pm 0.02$ cc/m^2.day) in the unprocessed state (Table 2), making them an excellent alternative to foil-based packaging. However, the OTRs of all the pouches increased significantly ($P < 0.05$) after thermal sterilization. The change was dependent on film structures and process severity (Table 2). MOA showed the highest change in OTR (by 26 times) after 30 min of processing while MOC showed least change (by two times) after processing. Additional layers of organic coating (Table 1) and the overlayer in MOC may have minimized the damage to the metal oxide coating during thermal processing, leading to lesser changes in the pouch OTR. The OTRs of the MOB and MOD pouches also showed significant change after processing ($P < 0.05$), but it was lesser than the MOA structure.

In metal oxide coated films, the activation energy required for oxygen permeation was observed to be similar to that of the uncoated polymeric films (Henry et al., 2001). This indicates that the mechanism of permeation is independent of any interaction with a specific barrier coating. Rather, it is based on permeation through the polymeric layers and the coating tends to work as a protective barrier, limiting oxygen permeation. Hence, any defects in the metal oxide coating would allow the oxygen to permeate through the polymer substrate (Henry et al., 2001). The gel system facilitated identification of regions with defects e.g., pinholes and cracks in the coating. As discussed in the following sections, SEM and CLSM images showed the presence of such defects on the pouches (Figure 2 to 8). Oxygen permeation is primarily dependent on macro defects (>1 nm) in metal oxide coatings (Roberts et al., 2002). It also increases with applied strain for thinner films once a certain threshold limit is reached, due to an increase in crack density (Yanaka et al., 2001). Additional coatings, for

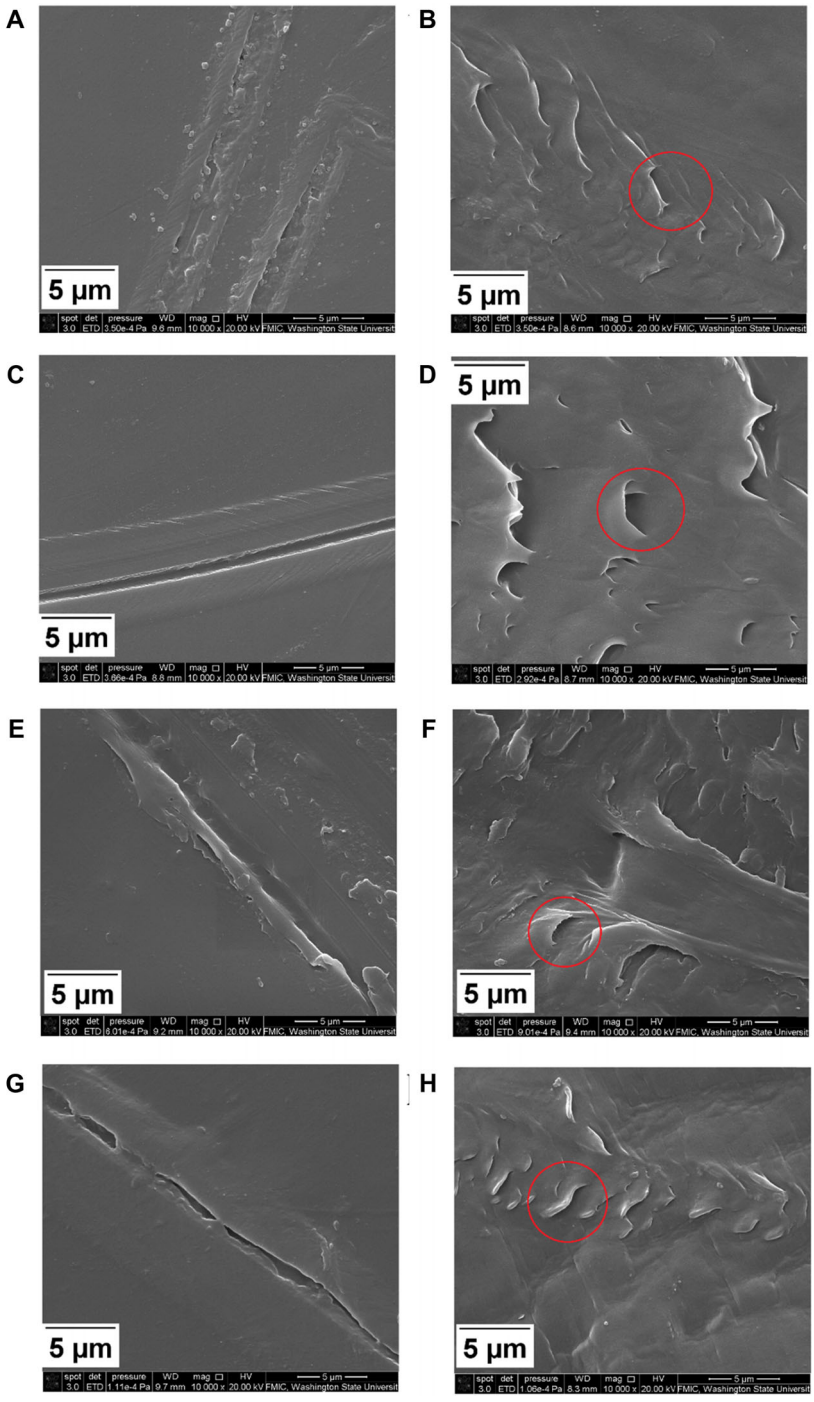

Figure 2–SEM micrographs of unprocessed (control) samples at 10000x after 180 days of storage at 23 °C with A, C, E, G representing the outer (PET) and B, D, F, H representing the inner (PP) sides of MOA, MOB, MOC, and MOD multilayer pouches, respectively. Locations with defects in PP layers are highlighted in red.

example, organic coating over the metal oxide layer, can reduce the defects in coated structures and thereby reduce the OTR (Singh et al., 2007).

In this study, we also found fewer cracks and pinholes (Figure 3 to 8) and a lower color change in gel for MOC pouch (Figure 1).This correlated well with its OTR after the thermal processing (Table 2). The organic coating in the MOC pouch contributed towards lowering the damage to the AlO_x coating, due to its crosslinking effect during sterilization (Singh et al., 2007). The presence of the overlayer also helped minimize defects. On the other hand, the MOA pouch with no organic coating or overlayer was more susceptible to developing defects after sterilization. Zhang et al., 2017 also reported an increase in OTR by 12 times for metal oxide coated films. This was due to processing-induced defects, in accordance with our results. The structural changes in polymers also contribute to reduction in gas barrier properties after thermal treatment. However, morphological changes have less influence on the barrier properties of metal oxide coated films than EVOH-based multilayer structures (Bhunia et al., 2016; Dhawan et al., 2014; Zhang et al., 2017). Nevertheless, several other factors that may have contributed to changes in film barrier properties include moisture absorption by

Table 2–Changes in OTRs and WVTRs of metal oxide coated pouches with thermal processing.

	OTR (cc/m^2. day) at 23 °C and 55 ± 1% RH			WVTR (g/m^2.day) at 38 °C and 100% RH		
Pouch type	Control	R30	R40	Control	R30	R40
MOA	0.04 ± 0.02^{bAB}	1.02 ± 0.72^{abA}	0.86 ± 0.18^{aA}	0.11 ± 0.01^{bC}	0.33 ± 0.02^{aA}	0.32 ± 0.08^{aB}
MOB	0.02 ± 0.01^{bA}	0.08 ± 0.03^{abA}	0.10 ± 0.01^{aB}	0.72 ± 0.06^{aA}	1.09 ± 0.5^{aA}	1.15 ± 0.5^{aAB}
MOC	0.02 ± 0.01^{bAB}	0.04 ± 0.01^{aA}	0.03 ± 0.01^{abC}	0.31 ± 0.02^{bB}	0.34 ± 0.04^{bA}	1.4 ± 0.07^{aA}
MOD	0.01 ± 0.01^{bB}	0.06 ± 0.01^{aA}	0.09 ± 0.02^{aB}	0.11 ± 0.01^{bC}	0.41 ± 0.13^{abA}	0.61 ± 0.11^{aB}

Note: The values are presented as Mean ± SD. Different lower-case and upper-case superscripts show significant differences ($P < 0.05$) between values within rows and columns, respectively. R30 and R40 correspond to 30 and 40 min of retort processing, respectively.

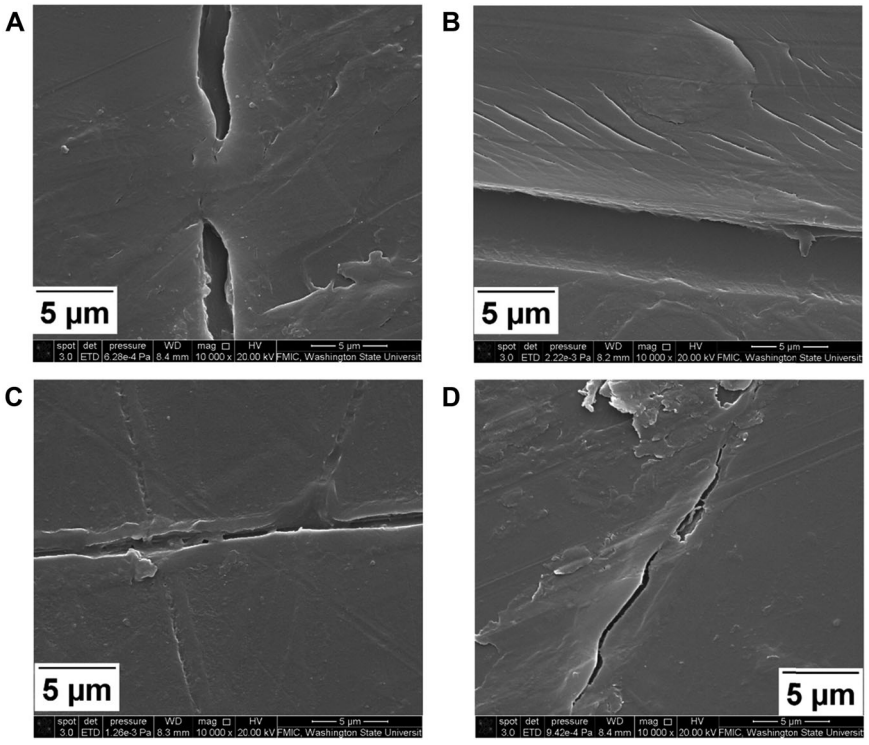

Figure 3–SEM micrographs of cracks at 10000x in outer (PET) side of processed pouches (R40) after 180 days of storage at 23 °C with A, B, C and D representing MOA, MOB, MOC, and MOD pouches, respectively.

hygroscopic nylon in the multilayer structure, an increase in free volume and the formation of smaller crystals with increasingly distorted crystal lattices (Bhunia et al., 2016; Zhang et al., 2017).

On the other hand, the WVTRs of MOA, MOC, and MOD increased significantly ($P < 0.05$) by 3, 5, and 6 times, respectively upon thermal processing of 40 min. There was no significant change in WVTRs of MOB ($P > 0.05$). The WVTR of MOC differed significantly ($P < 0.05$) from MOA and MOD before and after processing. The mechanism behind permeation of moisture in metal oxide coated films tended to differ from that of oxygen. Both the hydrophobic polypropylene layer and the metal oxide coating influence moisture barrier performance in multilayer films (Charifou et al., 2016; Zhang et al., 2017). The overall changes in WVTR of multilayer film may be due to the interaction between water molecules and the coating surface, as well as the presence of defects (Henry, Dinelli, Roberts, Kumar, & Howson, 1999).Therefore, moisture permeation is primarily dependent on the chemical interaction between the coating material and the water molecules (Henry et al., 1999, 2001), the surface contact angle of the moisture with respect to the type of coating used (Charifou et al., 2016), and the presence of nano-defects (Roberts et al., 2002; Struller et al., 2014). Having a homogeneous coating surface can also reduce the ingress of gasses and moisture through the films (Charifou et al., 2016).

Hence, barrier deterioration may be one of several factors that could have changed the WVTRs after thermal processing. It is also evident from Table 2 that MOC pouches with the least OTR had a comparatively higher WVTR. This can be attributed to the interaction between the coating material and moisture as MOC showed fewer defects. Although the gel method can only evaluate the barrier performance in terms of oxygen ingress, it still remains relevant as the size of an oxygen molecule is smaller than that of water (Roberts et al., 2002) and defects influence the OTRs of the films more than WVTRs.

Thermal analysis

The enthalpy of crystallinity of the polymeric films increased significantly ($P < 0.05$) after thermal processing (Table 3). In unprocessed pouches (control), all four structures had significantly different enthalpies of crystallinities ($P < 0.05$) with MOB pouches having the highest value. However, after 30 and 40 min of sterilization, there was no significant difference ($P > 0.05$) between the crystalline enthalpies of MOA and MOD, and, MOC and MOD pouches, respectively. However, the MOB structures were

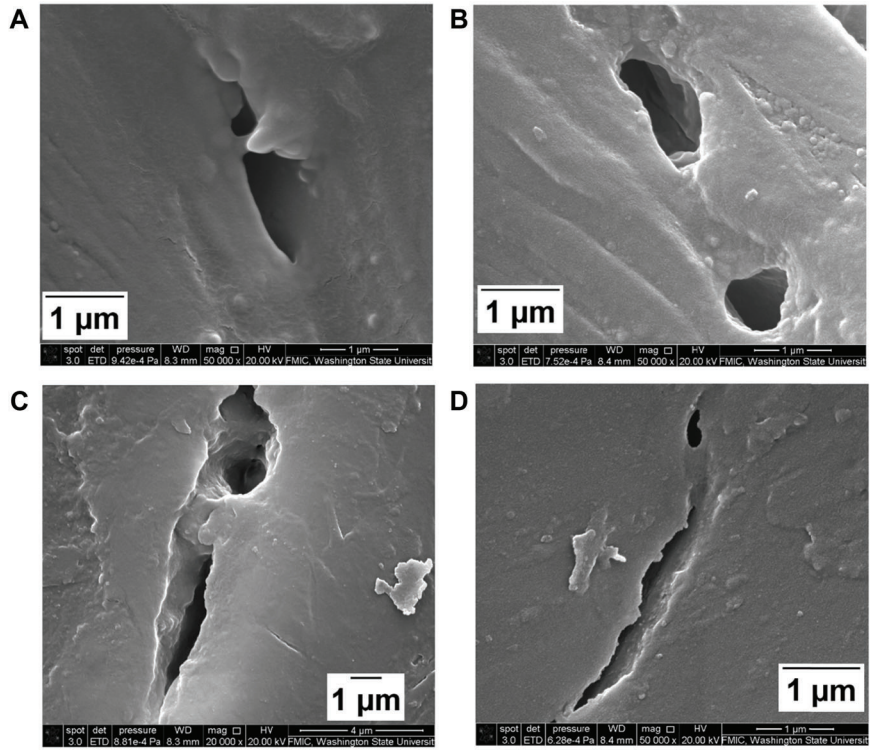

Figure 4–SEM micrographs of pinholes in outer (PET) side of processed pouches (R40) after 180 days of storage at 23 °C with A, B, C and D representing MOA, MOB, MOC, and MOD pouches, respectively.

Table 3–Change in enthalpy of crystallinity of metal oxide coated pouches with thermal processing.

	Enthalpy of crystallinity (ΔH, J/g)		
Pouch type	Control	R30	R40
MOA	47.8 ± 0.7^{cD}	56.9 ± 0.6^{bB}	60.1 ± 0.6^{aB}
MOB	56.9 ± 0.1^{cA}	60.3 ± 0.5^{bA}	63.9 ± 0.8^{aA}
MOC	50.5 ± 0.4^{cC}	52.3 ± 0.5^{bC}	55.8 ± 0.7^{aC}
MOD	52.2 ± 0.2^{cB}	55.3 ± 0.5^{bB}	58.3 ± 0.6^{aBC}

Note: The values are presented as Mean ± SD. Different lower-case and upper-case superscripts show significant differences ($P < 0.05$) between values within rows and columns, respectively. R30 and R40 correspond to 30 and 40 min of retort processing, respectively.

significantly different ($P < 0.05$) from MOA, MOC and SiO_x-coated MOD pouches. In addition, MOA pouches differed significantly ($P < 0.05$) from MOC pouches for both thermal treatments. Table 3 indicates that MOA pouches showed a change of 12.3 J/g in crystalline enthalpy, the highest amongst the four pouches. The MOB, MOC, and MOD structures observed changes of 7, 5.3, and 6.1 J/g, respectively. Unprocessed samples showed peaks for cold crystallization which decreased in all films after exposure to thermal processing at 121 °C.

The change in overall enthalpies of crystallinities in the films may be attributed to changes in chain structures of the polymers caused by the annealing effect induced by sterilization conditions under high moisture environment. In the case of PET and nylon, thermal processing can bring about changes to the molecular structure, resulting in enhanced crystallinity after thermal treatment (Bhunia et al., 2016; Dhawan et al., 2014; Zhang et al., 2017). The PET crystallinity decreased immediately after thermal processing or remained unchanged, while that of nylon increased (Dhawan et al., 2014; Zhang et al., 2017). This may have resulted in nylon losing its mechanical strength upon thermal processing, leading to a more brittle structure overall. With storage, PET crystallinity tends to increase, making it more brittle (Zhang et al., 2017).

It has also been reported that PET undergoes chemicrystallization, which involves chain scissions in its amorphous regions. This leads to the formation of smaller chains, increasing crystallinity and thereby brittleness (Bhunia et al., 2016). This may make the coating more prone to defects induced by mechanical stresses. Overall, using the gel method for detection of packaging defects facilitated the identification of affected sites in the metal oxide coating. Understanding the extent of changes in polymer crystallinity can lead to formulation of more suitable coating substrates.

Scanning electron microscopy

Between the four structures tested, MOA and MOB showed higher defects than those observed in MOC and MOD pouches (Figure 2 to 4). The MOB pouches showed comparatively lower defects than MOA pouches. The overlayer and organic coating in MOC and the overlayer in MOD may have minimized defects in the polymeric layers by filling up cracks and pinholes, in addition to the crosslinking effect provided by the organic coating (Singh et al., 2007). Results also show that MOB without an overlayer exhibited more defects than MOD with an overlayer, even though both of these films had an SiO_x-based coating. All of the structures showed an increase in magnitude of defects after thermal processing (Figure 2 to 4). Although SEM did not offer insight into the defects in the metal oxide layer itself, it did provide information related to changes in polymer surfaces.

Results show that all pouches developed pinholes (Figure 4) after exposure to high temperatures during thermal processing. In combination with cracks in the coatings, these pinholes may have contributed to the loss of barrier properties and an increase in

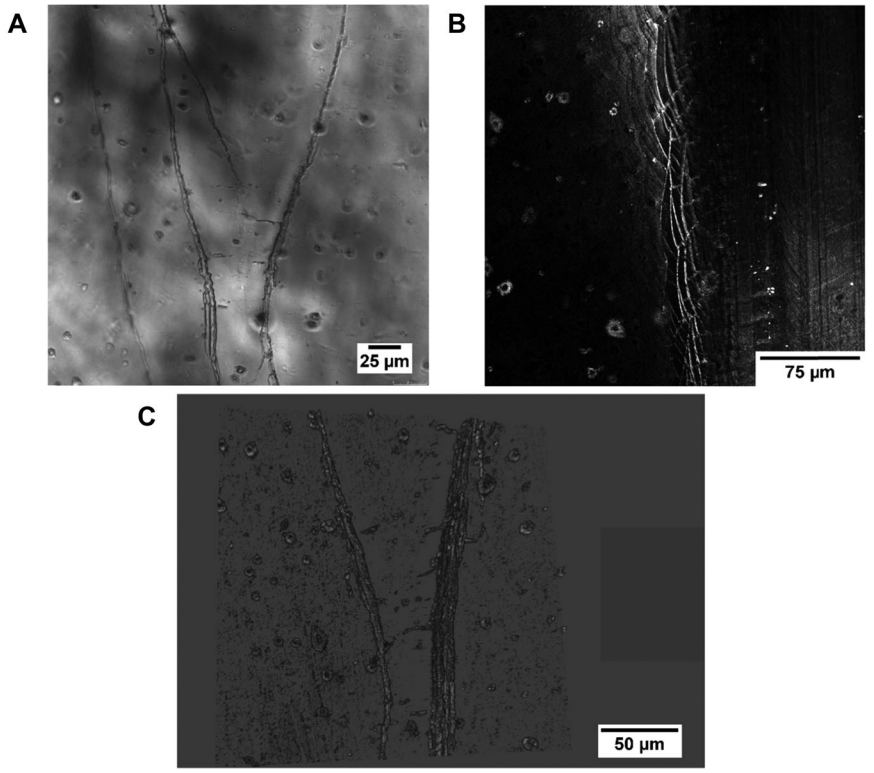

Figure 5–CLSM micrographs of unprocessed (control) MOA pouches (A) 2D view in transmittance mode after 180 days of storage at 23 °C, (B) 2D view in reflectance mode after 90 days of storage at 40 °C and (C) 3D view after 180 days of storage at 23 °C with the coating side to the front.

gas transmission rates after sterilization. SEM micrographs of the inner PP layer also showed defects (Figure 2). All four pouches had these defects for both retort processes (R30 and R40), as well as in unprocessed (control) pouches. This suggests that these formed during the co-extrusion and metal oxide coating processes, and not as a result of retort processing.

Other factors that may have contributed to defects in polymer layers were changes in polymeric chain structures induced by heat treatment and associated stresses. The polymeric layers are usually subjected to three major stresses during the coating process. This includes internal stresses such as shrinkage induced by changes in polymer crystallinity or recovery after deposition of coatings, thermal stresses from exposure to high heat during metal oxide coating, and lastly, stresses caused by intrinsic factors such as disorders related to the coating growth processes (Leterrier et al., 2001; Rochat et al., 2005).

In this study, SEM micrographs of unprocessed samples (Figure 2) indicated the presence of defects prior to thermal processing. This may be attributed to thermal and intrinsic stresses during the co-extrusion and coating stages. However, the increase in dimensions of these defects after thermal processing may be caused by internal stresses from expansion and shrinkage of polymers. The polymeric layers used in these pouches tended to be biaxially oriented in the unprocessed state. Upon heating above the glass transition temperature, these may have undergone shrinkage because of crystallization and chain relaxation. Rochat et al. (2005) reported that during heating, SiO_x-coated PET films expanded up to the glass transition temperature (T_g) and subsequently shrunk when heated up to 150 °C. The films shrunk again on cooling. The overall shrinkages in coated and uncoated PET were 0.73% and 0.67%, respectively with applied strain. Without this strain, the shrinkage was reported as 1.8% in coated films. This shrinkage was induced by chain relaxation rather than a change in crystallinity. Leterrier et al., 2001 also reported shrinkage in metal oxide coated PET structures upon heating. In this case, coated films showed less shrinkage than uncoated PET films. However, both the studies reported shrinkage upon annealing.

In this study, the crystallinity of the films increased significantly ($P < 0.05$) after thermal processing. This may have contributed to shrinkage in films resulting in defects. Other factors may include mechanical stresses during storage and handling and absorption of moisture by the polymeric materials such as nylon. Moisture absorption causes plasticization of the chains during thermal processing (Zhang et al., 2017). During the postprocessing stage, polymers may have released this excess moisture, reducing mechanical strength and increasing defects (Bhunia et al., 2016; Zhang et al., 2017).

Confocal laser scanning microscopy

CLSM analysis provided visualization of cracks and pinholes, as evident in 2D and 3D images (Figures 5 to 8). Pinholes were also observed near cracks, as shown in Figure 6 to 8. The MOA pouches had fewer pinholes and cracks in the unprocessed state (Figure 5). Similar observations were made for other structures. After processing, the cracks increased both in numbers and dimensions, and there were a greater number of pinholes as well (Figure 6 to 8). The coating layer in MOA exhibited more defects than other films at both 23 and 40 °C. It is notable that in CLSM micrographs, pinholes were less visible in 40 °C storage samples (Figure 7). Pouches stored at 40 °C showed development of an intense blue color, as explained in the earlier sections. This blue color prevented analysis of samples in transmittance mode, due to decreased penetration of the laser across the complete film thickness. However, cracks in pouches stored at 40 °C showed similar

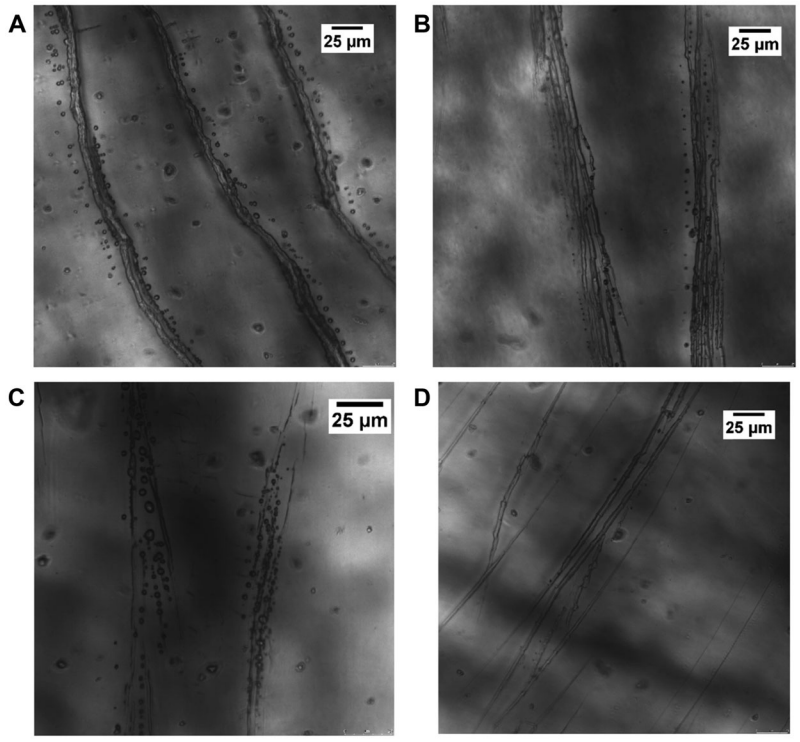

Figure 6–CLSM 2D micrographs of processed pouches (R40) (A) MOA, (B) MOB, (C) MOC, and (D) MOD after 180 days of storage at 23 °C in transmittance mode with the coating side to the front.

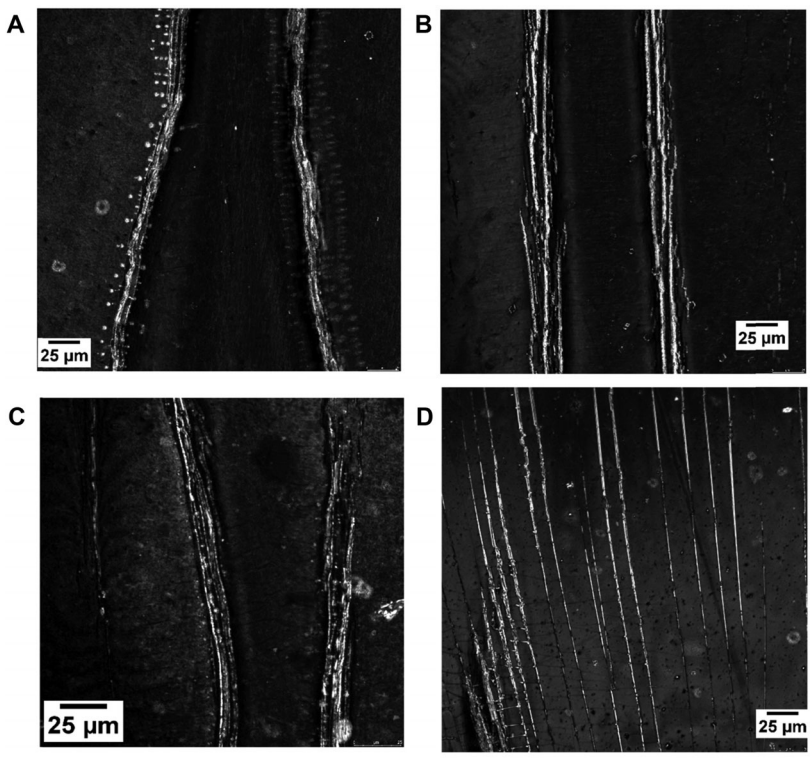

Figure 7–CLSM 2D micrographs of processed pouches (R40) (A) MOA, (B) MOB, (C) MOC, and (D) MOD after 90 days of storage at 40 °C in reflectance mode with the coating side to the front.

trends as the 23 °C samples (Figure 7). CLSM was also used to analyze the regions with no blue coloration, which showed no defects of any kind. This confirmed the effectiveness of the gel system (images not shown).

All metal oxide coated structures examined in this study showed defects prior to thermal processing. This was evident from the unprocessed (control) pouches stored at 23 and 40 °C for the same duration as the processed samples (Figure 1). These

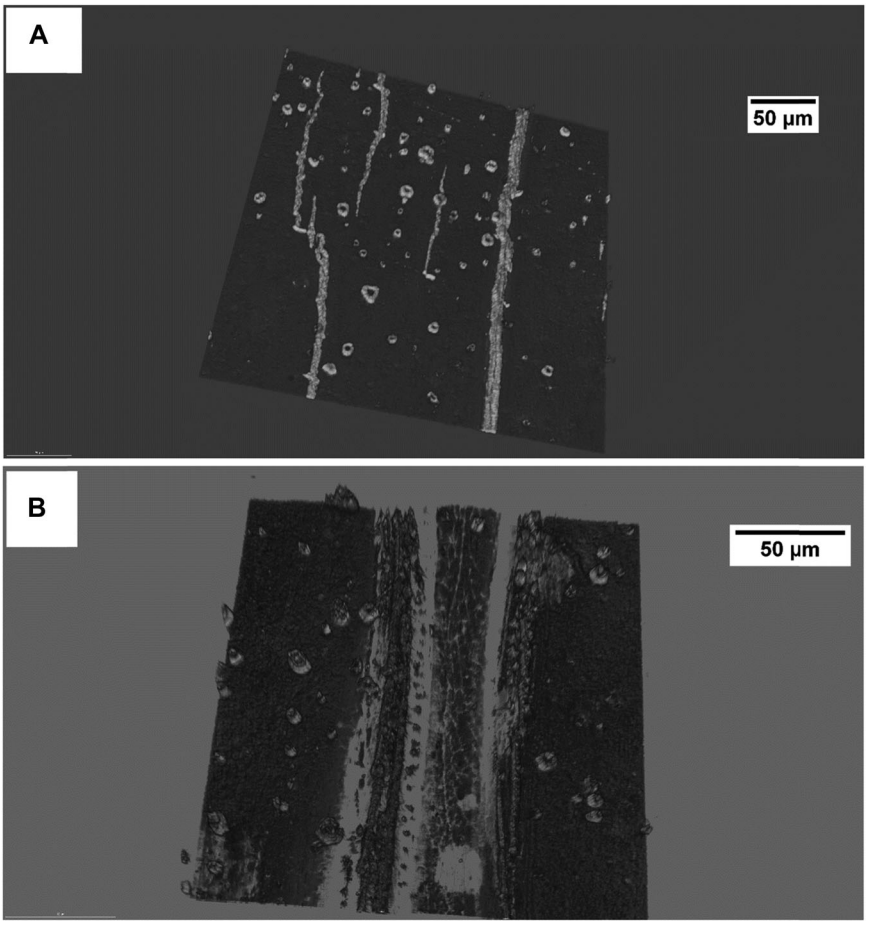

Figure 8–CLSM 3D micrographs of processed pouches (R40) (A) MOA, (B) MOC after 180 days of storage at 23 °C with the coating side to the front.

pre-processing defects are also seen in other polymer substrates such as AlO_x-coated, biaxially oriented PP (Struller et al., 2014). Other researchers have found similar results for metal oxide coating deposition through PVD or CVD techniques (Henry et al., 2001; Roberts et al., 2002; Yanaka et al., 2001). Upon exposure to thermal treatments, these existing deformities may have resulted in cracks and pinholes. Therefore, regardless of deposition method adopted or the substrate chosen, defects were observed.

However, a key factor is the thickness of the metal oxide coating applied. Dimensional changes such as shrinkage in the films vary with coating thickness for metal oxide coated structures. Specifically, films with thinner coatings have more shrinkage in polymer substrate as compared to thicker coatings (Rochat et al., 2005). This may increase the number of defects in the coating as well. The surface roughness of the polymer substrate also plays a vital role in inducing defects in the deposited coating. Antiblocking particles on the substrate may lead to defects such as voids in the metal oxide coating (Struller et al., 2014). Overall, the confocal analysis helped us identify the changes in the metal oxide coating layer located between polymeric layers that otherwise wouldn't not have been possible to characterize. Combined with the gel method to identify the locations of cracks and pinholes, this technique helped to shed light on the nature and type of defects present in metal oxide coated structures.

Conclusion

In this study, our novel gel system was sensitive enough to locate defects in metal oxide coated polymeric films due to its ability to change color with oxygen ingress. Changes in gel color and the presence of cracks and pinholes in pouches correlated well to changes in the OTRs of multilayer films. The presence of an organic coating and overlayer along with metal oxide coating minimized the loss of barrier properties due to thermal sterilization. In fact, pouches with such coatings performed better than those consisting of AlO_x or SiO_x coatings only. Using SEM and CLSM techniques, we characterized the nature of defects and confirmed the accuracy of gel method in identifying defects. Oxygen is the primary cause of deterioration in the shelf life of sterilized foods with polymeric packaging and in metal oxide coated films, the barrier performance depends on the coating integrity. This study is significant in terms of finding an effective method to assess the effects of thermal sterilization on coating performance. The gel system may facilitate further improvements in the development of metal oxide coated high barrier films for in-package sterilization processes.

Acknowledgments

This work was supported by the USDA National Inst. of Food and Agriculture Research grants #2016-67017-24597 and #2016-68003-24840. The authors would like to thank Mr. Frank

Younce, manager food processing pilot plant, FSHN, WSU and Drs. Valerie Lynch-Holm and Dan Mullendore of FMIC, WSU for their technical help. The authors would also like to thank the polymer companies for supplying the samples and Toppan USA, Inc. for helping us with the development of this gel.

Author Contributions

Ashutos Parhi designed and performed the experiments, collected and analyzed data and prepared a first draft of the manuscript. Kanishka Bhunia assisted in the design of experiments and preparation of gel-filled pouches, in interpretation of data, and contributed to editing the manuscript. Barbara Rasco and Juming Tang assisted in data interpretation and editing the manuscript. Shyam S. Sablani supervised the project and contributed in design of experiments, interpreting results and editing the manuscript. Authors declare no competing interests in this study.

References

Ackers, G. K., & Steere, R. L. (1962). Restricted diffusion of macromolecules through agar-gel membranes. *Biochimica et Biophysica Acta*, *59*(1), 137–149. https://doi.org/10.1016/0006-3002(62)90704-7

Bélaz-David, N., Decosterd, L. A., Appenzeller, M., Ruetsch, Y. A., Chioléro, R., Buclin, T., & Biollaz, J. (1997). Spectrophotometric determination of methylene blue in biological fluids after ion-pair extraction and evidence of its adsorption on plastic polymers. *European Journal of Pharmaceutical Sciences*, *5*(6), 335–345. https://doi.org/10.1016/S0928-0987(97)00061-4

Bhunia, K., Sablani, S. S., Tang, J., & Rasco, B. (2016). Non-invasive measurement of oxygen diffusion in model foods. *Food Research International*, *89*, 161–168. https://doi.org/10.1016/j.foodres.2016.07.015

Bhunia, K., Zhang, H., Liu, F., Rasco, B., Tang, J., & Sablani, S. S. (2016). Morphological changes in multilayer polymeric films induced after microwave-assisted pasteurization. *Innovative Food Science and Emerging Technologies*, *38*, 124–130. https://doi.org/10.1016/j.ifset.2016.09.024

Brown, Z. K., Fryer, P. J., Norton, I. T., & Bridson, R. H. (2010). Drying of agar gels using supercritical carbon dioxide. *The Journal of Supercritical Fluids*, *54*(1), 89–95.

Byun, Y., Bae, H. J., Cooksey, K., & Whiteside, S. (2010). Comparison of the quality and storage stability of salmon packaged in various retort pouches. *LWT - Food Science and Technology*, *43*(3), 551–555. https://doi.org/10.1016/j.lwt.2009.10.001

Byun, Y., Hong, S. I., Mangalassary, S., Bae, H. J., Cooksey, K., Park, H. J., & Whiteside, S. (2010). The performance of organic and inorganic coated retort pouch materials on the shelf life of ready-to-eat rice products. *LWT - Food Science and Technology*, *43*(6), 862–866. https://doi.org/10.1016/j.lwt.2010.01.009

Campbell, J. A. (1963). Kinetics—Early and often. *Journal of Chemical Education*, *40*(11), 578. https://doi.org/10.1021/ed040p578

Charifou, R., Espuche, E., Gouanvé, F., Dubost, L., & Monaco, B. (2016). SiOx and SiOxCzHw mono- and multi-layer deposits for improved polymer oxygen and water vapor barrier properties. *Journal of Membrane Science*, *500*, 245–254. https://doi.org/10.1016/j.memsci.2015.11.040

Dhawan, S., Varney, C., Barbosa-Cánovas, G. V., Tang, J., Selim, F., & Sablani, S. S. (2014). The impact of microwave-assisted thermal sterilization on the morphology, free volume, and gas barrier properties of multilayer polymeric films. *Journal of Applied Polymer Science*, *131*(12), 1–8. https://doi.org/10.1002/app.40376

Henry, B. M., Dinelli, F., Roberts, A. P., Kumar, R. S., & Howson, R. P. (1999). A microstructural study of transparent metal oxide gas barrier ®lms. *Thin Solid Films*, *6*

Henry, B. M., Erlat, A. G., McGuigan, A., Grovenor, C. R. M., Briggs, G. A. D., Tsukahara, Y., . . . Niijima, T. (2001). Characterization of transparent aluminium oxide and indium tin oxide layers on polymer substrates. *Thin Solid Films*, *382*(1–2), 194–201. https://doi.org/10.1016/S0040-6090(00)01769-7

Kaas, R. L., & Darby, D. (2010). An Oxygen Indicator for Assessment of Barrier Packaging, TAPPI-PLACE, Albuquerque, New Mexico USA, April 18–21: Retrieved from http://www.tappi.org/content/events/10place/papers/kaas.pdf

Leterrier, Y., Månson, J.-A. E., & Wyser, Y. (2001). Internal stresses and adhesion of thin silicon oxide coatings on poly(ethylene terephthalate). *Journal of Adhesion Science and Technology*, *15*(7), 841–865. https://doi.org/10.1163/15685610152540885

Mills, A. (2005). Oxygen indicators and intelligent inks for packaging food. *Chemical Society Reviews*, *34*(12), 1003. https://doi.org/10.1039/b503997p

Mohan, C. O., Ravishankar, C. N., Bindu, J., Geethalakshmi, V., & Srinivasa Gopal, T. K. (2006). Effect of Thermal Process Time on Quality of "Shrimp Kuruma" in Retortable Pouches and Aluminum Cans. *Journal of Food Science*, *71*(6), S496–S500. https://doi.org/10.1111/j.1750-3841.2006.00099.x

Nishinari, K., & Fang, Y. (2016). Sucrose release from polysaccharide gels. *Food & Function*, *7*(5), 2130–2146. https://doi.org/10.1039/C5FO01400J

Pernodet, N., Maaloum, M., & Tinland, B. (1997). Pore size of agarose gels by atomic force microscopy. *Electrophoresis*, *18*(1), 55–58. https://doi.org/10.1002/elps.1150180111

Roberts, A. P., Henry, B. M., Sutton, A. P., Grovenor, C. R. M., Briggs, G. A. D., Miyamoto, T., & Yanaka, M. (2002). Gas permeation in silicon-oxide/polymer (SiOx/PET) barrier films: Role of the oxide lattice, nano-defects and macro-defects. *Journal of Membrane Science*, *208*(1–2), 75–88. https://doi.org/10.1016/S0376-7388(02)00178-3

Rochat, G., Leterrier, Y., Fayet, P., & Månson, J.-A. E. (2005). Stress controlled gas-barrier oxide coatings on semi-crystalline polymers. *Thin Solid Films*, *484*(1–2), 94–99. https://doi.org/10.1016/j.tsf.2005.02.020

Singh, B., Bouchet, J., Rochat, G., Leterrier, Y., Månson, J.-A. E., & Fayet, P. (2007). Ultra-thin hybrid organic/inorganic gas barrier coatings on polymers. *Surface and Coatings Technology*, *201*(16–17), 7107–7114. https://doi.org/10.1016/j.surfcoat.2007.01.013

Struller, C. F., Kelly, P. J., & Copeland, N. J. (2014). Aluminum oxide barrier coatings on polymer films for food packaging applications. *Surface and Coatings Technology*, *241*, 130–137. https://doi.org/10.1016/j.surfcoat.2013.08.011

Walstra, P. (2003). *Physical chemistry of foods*. New York: Marcel Dekker.

Yanaka, M. H., Roberts, B. M., Grovenor, A. P., Briggs, C. R. M., Sutton, G. A. D., Miyamoto, A. P., . . . Chater, N. R. J. (2001). How cracks in SiOx-coated polyester films affect gas permeation. *Thin Solid Films*, *397*(1–2), 176–185. https://doi.org/10.1016/S0040-6090(01)01473-0

Zhang, H., Bhunia, K., Munoz, N., Li, L., Dolgovskij, M., Rasco, B., . . . Sablani, S. S. (2017). Linking morphology changes to barrier properties of polymeric packaging for microwave-assisted thermal sterilized food. *Journal of Applied Polymer Science*, *134*(44), 1–10. https://doi.org/10.1002/app.45481